

Kondo-lattice model: Application to the temperature-dependent electronic structure of EuO(100) films

R. Schiller, W. Müller,* and W. Nolting
 Lehrstuhl Festkörpertheorie, Institut für Physik,
 Humboldt-Universität zu Berlin,
 Invalidenstr. 110, 10115 Berlin, Germany
 (Dated: October 24, 2018)

We present calculations for the temperature-dependent electronic structure and magnetic properties of thin ferromagnetic EuO films. The treatment is based on a combination of a multiband-Kondo lattice model with first-principles TB-LMTO band structure calculations. The method avoids the problem of double-counting of relevant interactions and takes into account the correct symmetry of the atomic orbitals. We discuss the temperature-dependent electronic structures of EuO(100) films in terms of quasiparticle densities of states and quasiparticle band structures. The Curie temperature T_C of the EuO films turns out to be strongly thickness-dependent, starting from a very low value ($\simeq 15K$) for the monolayer and reaching the bulk value at about 25 layers.

PACS numbers: 75.50.Pp,73.20.At,75.70.Ak,71.15.-m

I. INTRODUCTION

A highly vivid field of research in current solid state physics aims at the intercorrelation between electronic and magnetic properties of materials. Special highlights in this respect include phenomena like the colossal magnetoresistance (CMR) effect observed in the manganites perovskites $T_{1-x}D_xMnO_3$ where T is a trivalent lanthanide ion such as La and D is a divalent alkaline-earth (e.g. Ca, Ba, Sr) ion¹. The interest is fueled by the prospect for applications in the fields of storage media and sensor technology. Interesting from an even more fundamental point of view is the intercorrelation of electronic and magnetic properties in the so-called ‘local-moment’ magnets, prototypically realized by the metallic rare earths Gd, Tb and Dy² and the insulating rare-earth compounds EuO and EuS³. Sometimes these materials are also denoted as ‘4f systems’ because a great part of their properties is due to the existence of a partially filled and highly localized 4f-shell belonging to the rare-earth ion. Strong screening by other closed electron shells keeps the Hund’s rules valid. According to these the 4f electrons couple to a finite moment which is strictly localized at the sites of the rare-earth ion (Eu^{2+} , Gd^{3+} , ...). While the purely magnetic properties of these materials are due to their localized ‘magnetic’ 4f electrons the conductivity properties are determined by the quasi-free electrons in rather broad (5d, 6s) conduction bands.

Many characteristic features of 4f systems follow from an intimate correlation between localized and itinerant electrons. This correlation leads, e.g., to a striking temperature dependence of the conduction band states induced by the magnetization state of the local moment system. First evidence for this has been found in 1964 by the discovery of the ‘red shift effect’ in EuO by Busch and Wachter³. The effect refers to a strong shift of the lower band edge to lower energies upon temperature cooling below T_C . A further striking effect being due to the mentioned induced temperature dependence is a metal-insulator transition observed in Eu-rich EuO⁴. The Eu-richness manifests itself in (2+)-charged oxygen vacancies. One of the two excesses electrons is thought to be tightly

bound to the vacancy while, because of the Coulomb repulsion, the other occupies an impurity level fairly close to the lower band edge. When cooling below T_C the band edge crosses the impurity level (‘red shift’) freeing therewith the excess electrons. A conductivity jump of up to 14 orders of magnitude has been observed.

Further effects result from the interaction of the band electron with collective excitations of the moment system. One of these is the creation of a new quasiparticle which is called ‘magnetic polaron’. It can be classified as a propagating electron dressed by a virtual cloud of excited magnons. The formation of magnetic polarons strongly influences the electronic structure of respective materials^{5,6,7}.

The influence between localized and itinerant electrons is of course of mutual character. That means that a finite band occupation has observable consequences for the moment system, too. The ferromagnetic order in Gd, e.g., can be explained only by indirect exchange coupling (RKKY) of the localized moments (spins) mediated by a spin polarization of the a priori non-magnetic conduction electrons. This RKKY-mechanism can excellently be monitored by inspecting the alloy $Eu_{1-x}Gd_xS$. Replacing the Eu^{2+} -ion in the ferromagnetic insulator EuS by a Gd^{3+} leads in a definite manner to a population of the conduction band without diluting the local moment system. The latter holds because Eu^{2+} and Gd^{3+} both have a half-filled 4f-shell $S = \frac{7}{2}$. That allows for a direct study of the carrier concentration dependence of the Curie temperature $T_C = T_C(n)$ ^{8,9}.

It is commonly accepted that the so called s-f model^{10,11} provides a good starting point for an at least qualitative understanding of the above properties of typical ‘local moment’ materials. Within the model they are traced back to an intraatomic, interband exchange interaction between localized and extended states. The same model has been extensively applied in the recent past to the CMR-materials. In the manganites the three almost localized $3d_{t_{2g}}$ -electrons couple to an $S = \frac{3}{2}$ -spin that is exchange-coupled to the somewhat more mobile $3d_{e_g}$ -electrons. In this context the s-f model is referred to as the ferromagnetic Kondo-lattice model (FKLM)^{12,13,14}.

The additive ‘ferromagnetic’ points to an exchange coupling which favors the parallel alignment of itinerant and localized spin. Without this additive the ‘normal’ Kondo-lattice model (KLM) is meant that differs from the FKLM only by a sign change of the coupling constant favoring therewith an antiparallel alignment. The latter version is considered a candidate for the extraordinary heavy-fermion physics¹⁵. In this paper we exclusively refer to the FKLM, which covers the above described 4f-systems and the manganites. While the 4f-systems surely belong to the weak-coupling region (exchange coupling much smaller than the bandwidth) the manganites are to be ascribed to the strong coupling limit.

A central aspect of our study which we are going to present in this paper is that of reduced dimensionality and its interplay with typical correlation effects. Magnetic phase transitions and electronic structures at surfaces and in thin films have attracted a lot of recent research work. One of the most remarkable magnetic phenomena observed in 4f-systems is the existence of a ferromagnetic surface at temperatures where the bulk material is already paramagnetic. This effect was first documented for the Gd(0001) surface by Weller et al.¹⁷ and since then has been measured by several groups with different experimental techniques. Depending on the used techniques and maybe on the cleanness of the applied surface Curie-temperature enhancements $\Delta T_C = T_C(\text{surface}) - T_C(\text{bulk})$ in between 17K and 60K have been found^{16,17,18}. However, the possibility of an enhanced surface Curie-temperature remains a matter of controversy. Donath et al.¹⁹ using spin-resolved photoemission did not find any indication for $\Delta T_C > 0$ at Gd(0001) surfaces. By careful analysis applying spin-polarized secondary-electron emission spectroscopy to surface magnetization measurements and magneto-optic Kerr effect to bulk magnetization measurements Arnold and Pappas²⁰ come to the same conclusion. With respect to a possible ΔT_C at Gd (also Tb) surfaces the existence of a Gd(0001) surface state seems to play a crucial role. Predicted by band structure calculations²¹ and simultaneously measured with photoemission^{22,23,24} in particular its temperature dependent induced exchange splitting has attracted attention²⁵. Is it ‘Stoner-like’ collapsing for $T \rightarrow T_C$ or does the splitting persist in the paramagnetic phase performing the demagnetization by a redistribution of spectral weight (‘spin-mixing behavior’)^{24,25}? It is an open question whether and how a surface state can cause an enhanced surface-Curie temperature. To get insight a calculation of the temperature-dependent electronic structure of the real (!) Gd-film would be required. For providing the clues to such a treatment of local-moment metals we present in this paper the methodical approach for dealing with local-moment semiconductor films, which are in addition interesting in themselves. The semiconducting 4f-systems EuO, EuS may be considered as ‘low-density limits’ of the metallic Gd. They have the same half-filled 4f-shell as Gd producing localized $S = \frac{7}{2}$ -spins. They differ by the carrier concentration n ($n = 0$ in EuO, EuS; $n \neq 0$ in Gd). We present in this paper the description of a real EuO-film of variable thickness. We are interested in the layer-dependent magnetic and electronic properties. For this purpose we combine a many-body treatment of the FKLM with a ‘first-principle’

electronic structure calculation. For the many-body part we use a ‘moment-conserving decoupling procedure’ (MCDA) the idea of which is developed in ref. 6 for the single-band bulk-FKLM. The reformulation for the special situation of a film geometry has been performed in⁷. We present here the generalization to a multi-band-FKLM film. As to the real EuO (100) film we combine the model calculation with a ‘tight-binding linear muffin tin orbital’ (TB-LMTO) band structure calculation to get temperature- and layer-dependent magnetizations, quasiparticle densities of states (Q-DOS) and quasiparticle band structures (Q-BS). We find for thicker films (≥ 20 monolayers) a surface state. Being of course unoccupied it nevertheless exhibits a temperature-dependent exchange splitting induced by exchange coupling to the magnetic 4f-moment system. We speculate that this surface state can be considered an analogous to the Gd-surface state mentioned above. Furthermore, we find some evidence that the temperature behavior of the EuO-surface state together with the red shift of the lower conduction band edge may close the 4f-5d gap in the \uparrow -spectrum giving rise to a surface-insulator-halfmetal-transition.

II. MULTIBAND-KONDO LATTICE MODEL

A. Model-Hamiltonian

We investigate a film consisting of n equivalent layers parallel to the surface of the film. Each lattice site of the film is indicated by a Greek letter $\alpha, \beta, \gamma, \dots$ denoting the layer index and a Latin letter i, j, k, \dots numbering the sites within a given layer. Each layer possesses two-dimensional translational symmetry. Accordingly, the thermodynamic average of any site dependent operator $A_{i\alpha}$ depends only on the layer index α :

$$\langle A_{i\alpha} \rangle \equiv \langle A_\alpha \rangle. \quad (1)$$

The complete d - f model Hamiltonian for a real system with multiple conduction bands,

$$\mathcal{H} = \mathcal{H}_d + \mathcal{H}_f + \mathcal{H}_{df}, \quad (2)$$

consists of three parts. The first

$$\mathcal{H}_d = \sum_{ij\alpha\beta\sigma} \sum_{mm'} T_{ij\alpha\beta}^{mm'} c_{i\alpha m\sigma}^+ c_{j\beta m'\sigma} \quad (3)$$

contains the conduction band structure of e.g. EuO. The indices m and m' denote the different conduction bands. $c_{i\alpha m\sigma}^+$ and $c_{i\alpha m\sigma}$ are, respectively the creation and annihilation operators of a spin- σ electron from the m 'th subband at the lattice site $\mathbf{R}_{i\alpha}$. $T_{ij\alpha\beta}^{mm'}$ are the hopping integrals which later have to be obtained from an LDA calculation.

Each lattice site $\mathbf{R}_{i\alpha}$ is occupied by a localized magnetic moment, represented by a spin operator $\mathbf{S}_{i\alpha}$. In the case of Eu and Gd the 4f shell is exactly half-filled and, because of Hund's rules, has its maximal magnetic moment of

$7 \mu_B$. These localized moments are described by an extended Heisenberg Hamiltonian

$$\mathcal{H}_f = \sum_{ij\alpha\beta} J_{ij}^{\alpha\beta} \mathbf{S}_{i\alpha} \mathbf{S}_{j\beta} + D_0 \sum_{i\alpha} (S_{i\alpha}^z)^2. \quad (4)$$

The first term is the original Heisenberg Hamiltonian with the exchange integrals $J_{ij}^{\alpha\beta}$. The second term introduces a symmetry-breaking single-ion anisotropy, which is necessary for film geometries to obtain a collective magnetic order at finite temperatures^{26,27}. Here, one has typically $D_0 \ll J_{ij}^{\alpha\beta}$.

The distinguishing feature of the single-band Kondo-lattice model (s-f or d-f model) is an intraatomic exchange between the conduction electrons and the localized f-spins. The form of the respective Hamiltonian in the case of multiple conduction bands can be derived from the general form of the on-site Coulomb interaction between electrons of different subbands.

$$\mathcal{H}_I = \frac{1}{2} \sum_{L_1 \dots L_4} \sum_{\sigma\sigma'} U_{L_1 \dots L_4} c_{L_1\sigma}^+ c_{L_2\sigma'}^+ c_{L_3\sigma'} c_{L_4\sigma} \quad (5)$$

We drop for the moment the site index i because we want to keep the local character of the s-f interaction. $L_1 \dots L_4$ denote the different bands, and $U_{L_1 \dots L_4}$ are the Coulomb matrix elements. Restricting the electron scattering processes caused by the Coulomb interaction to two involved subbands we get instead of (6):

$$\begin{aligned} \mathcal{H}_I = \frac{1}{2} \sum_{L,L'} \sum_{\sigma\sigma'} [& U_{L,L'} c_{L\sigma}^+ c_{L'\sigma'}^+ c_{L'\sigma'} c_{L\sigma} + \\ & J_{L,L'} c_{L\sigma}^+ c_{L'\sigma'}^+ c_{L'\sigma'} c_{L\sigma} + \\ & J_{L,L'}^* c_{L\sigma}^+ c_{L'\sigma'}^+ c_{L'\sigma'} c_{L\sigma}] \quad (6) \end{aligned}$$

Thinking of 4f systems such as EuO and Gd the band indices L and L' can be attributed either to a flat 4f band ($L \rightarrow f$) or to a broad (5d,6s) conduction band ($L \rightarrow m$). In an obvious manner we can then split the Coulomb interaction into three different parts

$$\mathcal{H}_I = \mathcal{H}_I^{cc} + \mathcal{H}_I^{ff} + \mathcal{H}_I^{cf} \quad (7)$$

depending on whether both interacting particles stem from a conduction band, \mathcal{H}_I^{cc} , or both from a flat band, \mathcal{H}_I^{ff} , or one from a flat band the other from a conduction band, \mathcal{H}_I^{cf} . The first term refers to electron correlations in the conduction bands, which by definition is neglected in the KLM. In the case of EuO this simplification becomes exact because the conduction bands are unoccupied ($n = 0$). On the other hand, for the CMR-materials the neglect of \mathcal{H}_I^{cc} appears questionable. Some authors therefore extend the KLM to the ‘correlated’ KLM by regarding \mathcal{H}_I^{cc} as the Hubbard-interaction²⁸. The second term, \mathcal{H}_I^{ff} , is already contained in the description of the localized moments via the Heisenberg model (4). So we are left with the interaction between localized and itiner-

ant electrons:

$$\begin{aligned} \mathcal{H}_I^{cf} = \sum_{m,f,\sigma,\sigma'} [& U_{mf} c_{m\sigma}^+ c_{f\sigma'}^+ c_{f\sigma'} c_{m\sigma} + \\ & J_{mf} c_{m\sigma}^+ c_{f\sigma'}^+ c_{m\sigma'} c_{f\sigma} + \\ & \frac{1}{2} J_{mf}^* c_{m\sigma}^+ c_{m\sigma'}^+ c_{f\sigma'} c_{f\sigma} + \\ & \frac{1}{2} J_{mf}^* c_{f\sigma}^+ c_{f\sigma'}^+ c_{m\sigma'} c_{m\sigma}] \quad (8) \end{aligned}$$

The last two terms do not contribute in case of the 4f systems (EuO,Gd) since the (Eu^{2+}, Gd^{3+})-4f shell has its maximum spin of $S = \frac{7}{2}$. All the seven 4f electrons have to occupy different subbands and none of the 7 sublevels will be doubly occupied. Introducing electron spin operators,

$$\begin{aligned} \sigma^+ &= \hbar c_{\uparrow}^+ c_{\downarrow} \\ \sigma^- &= \hbar c_{\downarrow}^+ c_{\uparrow} \\ \sigma^z &= \frac{\hbar}{2} (n_{\uparrow} - n_{\downarrow}) \quad (9) \end{aligned}$$

one arrives at

$$\begin{aligned} \mathcal{H}_I^{cf} &= -\frac{2}{\hbar^2} \sum_{mf} J_{mf} \sigma_m \sigma_f + \\ &+ \sum_{mf} (U_{mf} - \frac{1}{2} J_{mf}) n_m n_f \quad (10) \end{aligned}$$

with $n_{m(f)} = n_{m(f)\uparrow} - n_{m(f)\downarrow}$. In the case of EuO, we are interested in, the last term does not contribute because of $n_m = 0$. Even for Gd ($n_m \neq 0$) it certainly can be neglected since the number of electrons is fixed, n_f thus being only a c-number. By defining the spin operator \mathbf{S} of the local f-moment,

$$\mathbf{S} = \sum_f \sigma_f \quad (11)$$

and by assuming the interband exchange J_{mf} to be independent on the band indices m and f ,

$$J_{mf} \equiv -\frac{1}{2} \hbar J \quad (12)$$

the interaction term eventually reads,

$$\mathcal{H}_I^f = -\frac{J}{\hbar} \sum_m \sigma_m \mathbf{S} \quad (13)$$

Reintroduction of the lattice site dependence ($R_{i\alpha}$) we end up with the interaction term of the multiband-KLM:

$$\begin{aligned} \mathcal{H}_{df} &= -\frac{J}{\hbar} \sum_{i\alpha m} \sigma_{i\alpha m} \mathbf{S}_{i\alpha} \\ &= -\frac{1}{2} J \sum_{i\alpha m \sigma} [z_{\sigma} \mathbf{S}_{i\alpha}^z + \\ &+ \mathbf{S}_{i\alpha m}^{\sigma} c_{i\alpha m-\sigma}^+ c_{i\alpha m \sigma}] \quad (14) \end{aligned}$$

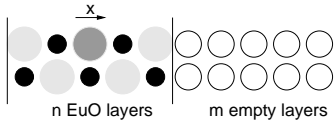


FIG. 1: Supercell geometry for the EuO(100) film calculations, with the Europium atoms (large), the oxygen atoms (small) and the empty spheres (circles). The vertical lines indicate the surface of the EuO film.

Here we have used the abbreviations

$$\begin{aligned} \mathbf{S}_{j\alpha m}^\sigma &= \mathbf{S}_{j\alpha m}^x + i z_\sigma \mathbf{S}_{j\alpha m}^y \\ z_\sigma &= \delta_{\sigma\uparrow} - \delta_{\sigma\downarrow} \end{aligned} \quad (15)$$

Compared to the conventional single-band KLM we have simply an additional band-summation in the exchange term. Note, however, the subbands are intercorrelated via the single-particle term \mathcal{H}_d (3).

B. Band structure calculations

The hopping integrals $T_{ij\alpha\beta}^{mm'}$ in the single-particle Hamiltonian (3) has to contain the influences of all those interactions which are not directly covered by our model-Hamiltonian. For this reason we perform a band structure calculation according to the ‘tight binding’-LMTO-ASA program of Anderson^{29,30}. The resulting single-particle energies are taken as single-particle input for the partial Hamiltonian (3).

Test calculations for bulk-EuO have revealed the well known ‘gap problem’ which appears in connection with the strongly localized character of the 4f-‘bands’. A ‘normal’ LDA calculation makes EuO a metal with the 4f-levels lying well within the conduction band. To overcome this situation we have investigated two approaches for dealing with the localized 4f moments (see³¹ for the analogous case of Gd). In the first, the 4f moments are treated as localized core electrons, which naturally gives an insulator ground state, while the conduction band region consists predominantly of Eu-5d states. In the second, an LDA+U calculation^{32,33} has been performed, which has the advantage compared to the former procedure, that the flat 4f bands explicitly appear right between the O-2p bands and the Eu-5d bands. In this approach, a meanfield approximation for the direct Coulomb U and the exchange interaction between the 4f electrons is added to the LDA-energy functional. The parameters U and J can be used to position the 4f levels correctly in the band gap between the O-2p and the Eu-5d levels. Besides the fact, that adjustable parameters U and J somehow corrupt the idea of a ‘first principles’ calculation, and since we consider the 4f-levels in our model study only as localized magnetic moments (4), the much simpler LDA calculation has to be preferred in particular when our study focuses on more complicated film geometries. For the band-structure calculations- for EuO films one has to employ a supercell geometry as depicted in Fig. 1. As a result, the system has a super-layered structure with super-layers consisting of n consecutive EuO(100) layers followed

by m layers of empty spheres. That means, we have a system of periodically stacked EuO n-layer films, isolated from each other by m layers of empty spheres.

The number m of empty layers has to be chosen large enough to have truly isolated EuO films, but on the other hand also as small as possible to cut down on the numerical effort. In Fig. 2, the 5d-partial density of states of EuO(100) monolayers (n=1) is displayed for different numbers m of spacer layers. The DOS of the EuO monolayer converges quite quickly as a function of m. For the following we have chosen m=5 which, according to Fig. 2, seems to be a reasonable approximation for the case of ideally isolated EuO films ($m \rightarrow \infty$). Fig. 3. shows the partial densities of states of the

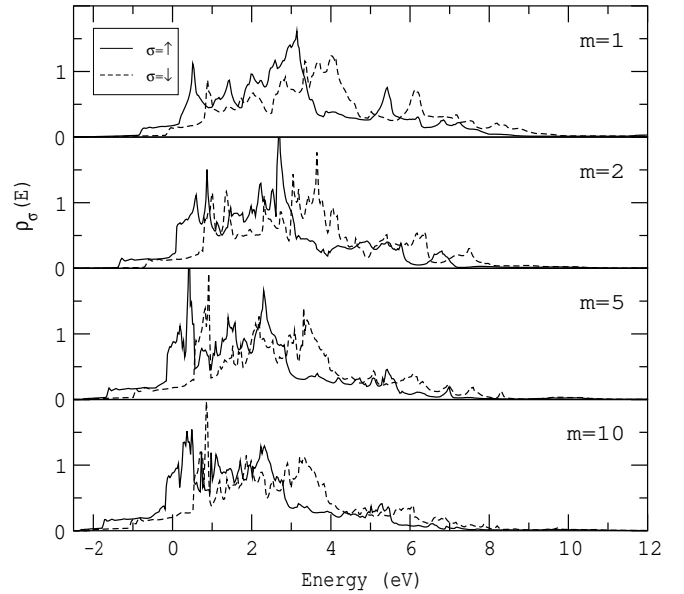


FIG. 2: Partial densities of states for the Eu-5d bands of a EuO(100) monolayer calculated for different numbers m of spacer layers of empty spheres.

5d bands of the center layer of films of various thicknesses and for bulk EuO. The respective curves converge as a function of film thickness. Comparing the partial Eu-5d DOS of the center layer ($\alpha = 10$) of a 20-layer EuO(100) film with that of bulk EuO, we see that apart from an unimportant constant energy shift the main features of the densities of states match. Consequently, the center layer at the 20-layer film can be regarded as a bulk-like environment. The still existing slight discrepancy may be accounted for by the fact that the supercell geometry in the band structure calculations for the EuO films destroys the cubic symmetry present in bulk EuO. Therefore, the splitting of the d-states into t_{2g} and e_g orbitals is not valid anymore. Furthermore, the center of a 20-layer EuO(100) film of course can be only an approximation in bulk EuO. Thus we believe that the slight discrepancy between the partial Eu-5d densities of states of the center layer of the 20-layer film and of bulk EuO is acceptable.

In Fig. 4 the partial Eu-5d densities of states of a 20-layer film are displayed for the two surface layers, $\alpha = 1, 2$, and for the two center layers, $\alpha = 9, 10$. We see that the local

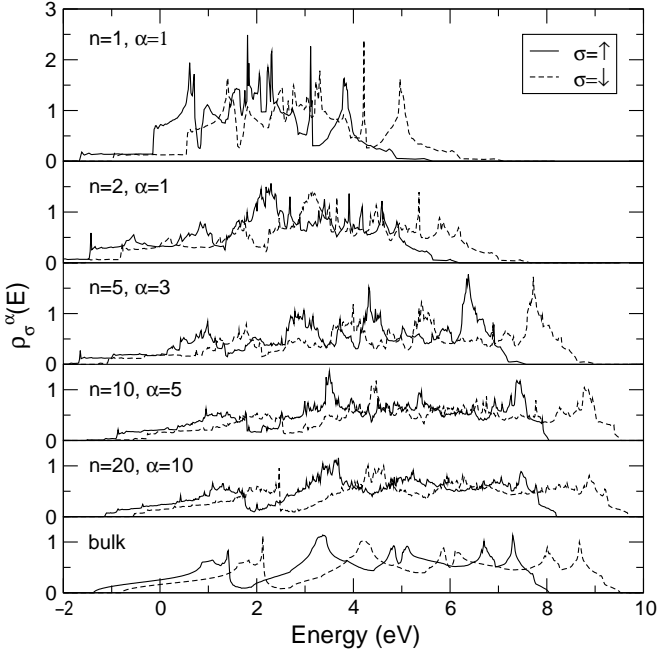


FIG. 3: Partial densities of states for the Eu-5d bands of the center layers (α : layer index) for EuO films of various thicknesses n . Bottom: Bulk EuO

density of states in the center of the film is constant, but different from that in the vicinity of the surface of the film. The lower band edge of the Eu-5d bands of the surface layer compared to those of the center layer, which represent a bulk-like situation, indicates the existence of surface states³⁴. This interesting point will be discussed a little bit later. When we take the results of the just-described band structure calculation as input for our finite temperature quasiparticle band structure calculation, then we are running into the well known ‘double counting problem’ of just the relevant interactions, once explicitly in the model-Hamiltonian and besides that implicitly in the above band structure calculation. How we avoid this problem is explained in the next Section.

III. MANY-BODY EVALUATION

After having fixed the model-Hamiltonian (2) and its renormalized single-particle energies in (3) via a full band structure calculation we have now to solve the many-body problem provoked by the Hamiltonian H . There are two partial problems to be solved, one concerning the magnetic properties of the localized 4f moments, the other dealing with the temperature-reaction of the conduction band states on the magnetic state of the moment system. Since we are interested in the description of the ferromagnetic semiconductor EuO, we can assume an empty conduction band ($n=0$), more strictly, a single electron in otherwise empty conduction bands. Therefore, the magnetic order cannot be influenced by conduction electrons and the magnetic part can be solved separately.

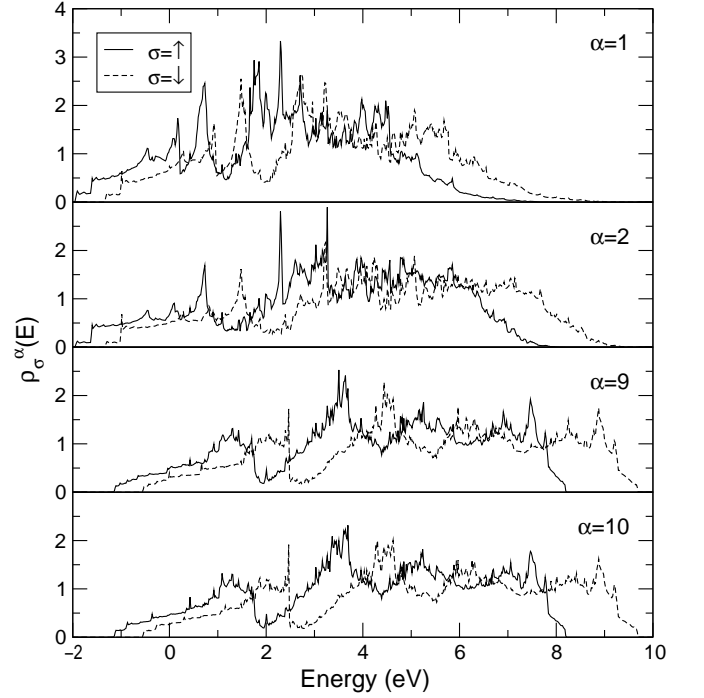


FIG. 4: Partial densities of states for the Eu-5d bands for different layers α of a 20-layer EuO(100) film.

A. Local moment system

The system of localized f -moments is described by the extended Heisenberg Hamiltonian (4). Here we want to stress once more that the single-ion anisotropy constant D_0 is small compared to the Heisenberg exchange interaction, $D_0 \ll J_{ij}^{\alpha\beta}$. By defining the magnon Green function

$$P_{ij}^{\alpha\beta}(E) = \left\langle\left\langle S_{i\alpha}^+; S_{j\beta}^- \right\rangle\right\rangle_E, \quad (16)$$

we can calculate the f -spin correlation functions by evaluating the equation of motion

$$E P_{ij}^{\alpha\beta}(E) = 2\hbar^2 \delta_{\alpha\beta} \langle S_\alpha^z \rangle + \left\langle\left\langle [S_{i\alpha}^+, \mathcal{H}_f]_-; S_{j\beta}^- \right\rangle\right\rangle_E. \quad (17)$$

The evaluation of this equation of motion involves the decoupling of the higher Green functions on its right-hand side, originating from the Heisenberg exchange term, and the anisotropy term using the Random Phase Approximation (RPA) and a decoupling proposed by Lines³⁵, respectively. The details of the calculation can be found in a previous paper³⁶. For brevity we restrict ourselves to present here only the results. For the layer-dependent magnetizations of the f -spin system we get³⁷

$$\frac{\langle S_\alpha^z \rangle}{\hbar} = \frac{(1 + \varphi_\alpha)^{2S+1} (S - \varphi_\alpha) + \varphi_\alpha^{2S+1} (S + 1 + \varphi_\alpha)}{\varphi_\alpha^{2S+1} - (1 + \varphi_\alpha)^{2S+1}}, \quad (18)$$

where

$$\varphi_\alpha = \frac{1}{N} \sum_{\mathbf{k}} \sum_{\gamma} \frac{\chi_{\alpha\alpha\gamma}(\mathbf{k})}{e^{\beta E_\gamma(\mathbf{k})} - 1}, \quad (19)$$

where, again, N is the number of sites per layer and $\beta = \frac{1}{k_B T}$. The summation \sum_{γ} in Eq. (19) runs over the n poles $E_\gamma(\mathbf{k})$ of the Green function $P_{\mathbf{k}}^{\alpha\beta}(E)$ and the $\chi_{\alpha\alpha\gamma}(\mathbf{k})$ is the weight of the γ 'th pole in the diagonal element of the Green function $P_{\mathbf{k}}^{\alpha\alpha}(E)$. The poles and the weights can be calculated from the RPA solution of Eq. (17):

$$P_{\mathbf{k}}^{\alpha\beta}(E) = 2\hbar^2 \begin{pmatrix} \langle S_1^z \rangle & & 0 \\ & \ddots & \\ 0 & & \langle S_n^z \rangle \end{pmatrix} \cdot (E\mathbf{I} - \mathbf{A})^{-1}, \quad (20)$$

with

$$\frac{(\mathbf{A})^{\alpha\beta}}{\hbar} = (D_0\Phi_\alpha + 2 \sum_{\gamma} J_0^{\alpha\gamma} \langle S_\gamma^z \rangle) \delta_{\alpha\beta} - 2J_{\mathbf{k}}^{\alpha\beta} \langle S_{\mathbf{k}}^z \rangle. \quad (21)$$

The Φ_α come from the decoupling of the higher Green function on the right-hand side of Eq. (17) and originates from the anisotropy term in the Hamiltonian \mathcal{H}_f according to Lines³⁵:

$$\Phi_\alpha = \frac{2\hbar^2 S(S+1) - 3\hbar \langle S_\alpha^z \rangle (1 + 2\varphi_\alpha)}{\langle S_\alpha^z \rangle}. \quad (22)$$

Having obtained the layer-dependent magnetizations (18) and the φ_α we can now express all the other f -spin correlation functions which we need for the following via the relations

$$\langle S_\alpha^- S_\alpha^+ \rangle = 2\hbar \langle S_\alpha^z \rangle \varphi_\alpha, \quad (23a)$$

$$\langle (S_\alpha^z)^2 \rangle = \hbar^2 S(S+1) \langle S_\alpha^z \rangle (1 + 2\varphi_\alpha), \quad (23b)$$

$$\begin{aligned} \langle (S_\alpha^z)^3 \rangle &= \hbar^3 S(S+1) \varphi_\alpha \\ &\quad + \hbar^2 \langle S_\alpha^z \rangle (S(S+1) + \varphi_\alpha) \\ &\quad - \hbar \langle (S_\alpha^z)^2 \rangle (1 + 2\varphi_\alpha), \end{aligned} \quad (23c)$$

and the general spin-operator equality

$$S_{i\alpha}^\sigma S_{i\alpha}^{-\sigma} = \hbar^2 S(S+1) + z_\sigma \hbar S_{i\alpha}^z - (S_{i\alpha}^z)^2. \quad (24)$$

We shall see in the next Section that these f -spin correlation functions provide the whole temperature dependence of the electronic subsystem (25).

B. Conduction bands

Similarly as the magnetic part in the preceding Section the electronic part can be treated separately in the case of EuO. The reason is that magnon energies and exchange integrals, respectively, are smaller by some orders of magnitude than other energies in the system as the d-f exchange J or the conduction band width W . Accordingly, the respective terms ($J_{ij}^{\alpha\beta}$, D_0) can be neglected when dealing with the electronic excitation

spectra. That does not at all mean that there is no influence of the magnetic moments on the electronic quasiparticle spectrum. That is done by the spin correlation functions of the last Section.

Starting from the Hamiltonian of the electronic subsystem,

$$\mathcal{H}^* = \mathcal{H}_d + \mathcal{H}_{df}, \quad (25)$$

all physical relevant information of the system can be derived from the retarded single-electron Green function:

$$\begin{aligned} G_{ij\alpha\beta\sigma}^{mm'}(E) &= \left\langle \left\langle c_{i\alpha m\sigma}; c_{j\beta m'\sigma}^+ \right\rangle \right\rangle_E \\ &= -i \int_0^\infty dt e^{-\frac{i}{\hbar}Et} \left\langle \left[c_{i\alpha m\sigma}(t), c_{j\beta m'\sigma}^+(0) \right]_+ \right\rangle. \end{aligned} \quad (26)$$

Here and in what follows $[\cdot, \cdot]_+$ ($[\cdot, \cdot]_-$) is the anticommutator (commutator). Conform to the two-dimensional translational symmetry, we perform a Fourier transformation within the layers of the film,

$$G_{\mathbf{k}\alpha\beta\sigma}^{mm'}(E) = \frac{1}{N} \sum_{ij} e^{i\mathbf{k}(\mathbf{R}_i - \mathbf{R}_j)} G_{ij\alpha\beta\sigma}^{mm'}(E), \quad (27)$$

where N is the number of sites per layer, \mathbf{k} is an in-plane wavevector from the first 2D-Brillouin zone of the layers and \mathbf{R}_i represents the in-plane part of the position vector, $\mathbf{R}_{i\alpha} = \mathbf{R}_i + \mathbf{r}_\alpha$. From Eq. (27) we get the spectral density by

$$S_{\mathbf{k}\alpha\beta\sigma}^{mm'}(E) = -\frac{1}{\pi} \text{Im} G_{\mathbf{k}\alpha\beta\sigma}^{mm'}(E + i0^+), \quad (28)$$

which is directly related to observable quantities within angle and spin resolved direct and inverse photoemission experiments. Finally, the wave-vector summation of $S_{\mathbf{k}\sigma}^{mm}(E)$ yields the layer-dependent (local) quasiparticle density of states:

$$\rho_{\alpha\sigma}^m(E) = \frac{1}{\hbar N} \sum_{\mathbf{k}} S_{\mathbf{k}\alpha\sigma}^{mm}(E). \quad (29)$$

In the following discussion all results will be interpreted in terms of the spectral density (28) and the local density of states (29).

For the solution of the many-body problem posed by Eq. (25) we write down the equation of motion of the single-electron Green function (26)

$$\begin{aligned} E G_{ij\alpha\beta\sigma}^{mm'} &= \hbar \delta_{ij} \delta_{\alpha\beta} \delta_{mm'} \\ &\quad + \sum_{k\gamma m''} T_{ik\alpha\gamma}^{mm''} G_{kj\gamma\beta\sigma}^{m''m'} \\ &\quad + \left\langle \left[c_{i\alpha m\sigma}, \mathcal{H}_{df} \right]_-; c_{j\beta m'\sigma}^+ \right\rangle_E. \end{aligned} \quad (30)$$

The formal solution of Eq. (30) can be found by introducing the self-energy $M_{ij\alpha\beta\sigma}^{mm'}(E)$,

$$\begin{aligned} \left\langle \left[c_{i\alpha m\sigma}, \mathcal{H}_{df} \right]_-; c_{j\beta m'\sigma}^+ \right\rangle_E &= \\ \sum_{k\gamma m''} M_{ik\alpha\gamma}^{mm''}(E) G_{kj\gamma\beta\sigma}^{m''m'}(E), \end{aligned} \quad (31)$$

which contains all information about the correlations between the conduction band and localized moments. After combining Eqs. (30) and (31) and performing a two-dimensional Fourier transform we see that the formal solution of Eq. (30) is given by

$$\mathbf{G}_{\mathbf{k}\sigma}(E) = \hbar (E \mathbf{I} - \mathbf{T}_{\mathbf{k}} - \mathbf{M}_{\mathbf{k}\sigma}(E))^{-1}. \quad (32)$$

Here, \mathbf{I} represents the $(nM \times nM)$ identity matrix, with M denoting the number of subbands of the conduction band system, and the matrices $\mathbf{G}_{\mathbf{k}\sigma}(E)$, $\mathbf{T}_{\mathbf{k}}$, and $\mathbf{M}_{\mathbf{k}\sigma}(E)$ have as elements the layer- and subband-dependent functions $G_{\mathbf{k}\alpha\beta\sigma}^{mm'}(E)$, $T_{\mathbf{k}\alpha\beta}^{mm'}$, and $M_{\mathbf{k}\alpha\beta\sigma}^{mm'}(E)$, respectively.

To explicitly get the self-energy in Eq. (31) we evaluate the Green function

$$\begin{aligned} & \left\langle \left\langle [c_{i\alpha m\sigma}, \mathcal{H}_{df}]_- ; c_{j\beta m'\sigma}^+ \right\rangle \right\rangle_E = \\ & -\frac{J}{2} \left(z_\sigma \Gamma_{ij\alpha\alpha\beta\sigma}^{mm'} + F_{ij\alpha\alpha\beta\sigma}^{mm'} \right). \end{aligned} \quad (33)$$

Here, the two higher Green functions,

$$\Gamma_{ikj\alpha\gamma\beta\sigma}^{m''m'}(E) = \left\langle \left\langle S_{i\alpha}^z c_{k\gamma m''\sigma}; c_{j\beta m'\sigma}^+ \right\rangle \right\rangle_E, \quad (34)$$

$$F_{ikj\alpha\gamma\beta\sigma}^{m''m'}(E) = \left\langle \left\langle S_{i\alpha}^{-\sigma} c_{k\gamma m''-\sigma}; c_{j\beta m'\sigma}^+ \right\rangle \right\rangle_E, \quad (35)$$

originate from the two terms of the d - f Hamiltonian (14) and will be referred to as the *Ising* and the *Spin-flip* function, respectively. Considering the equations of motion for these two Green functions we encounter the two higher Green functions $\left\langle \left\langle [S_{i\alpha}^z c_{k\gamma m''\sigma}, \mathcal{H}_{df}]_- ; c_{j\beta m'\sigma}^+ \right\rangle \right\rangle_E$ and $\left\langle \left\langle [S_{i\alpha}^{-\sigma} c_{k\gamma m''-\sigma}, \mathcal{H}_{df}]_- ; c_{j\beta m'\sigma}^+ \right\rangle \right\rangle_E$. Since we consider an empty conduction band the thermodynamic average in the Green functions has to be computed with the electron vacuum state $|n=0\rangle$. From the definition of the d - f Hamiltonian (14) we then see that $\langle n=0 | \mathcal{H}_{df} = 0$ and, accordingly,

$$\begin{aligned} & \left\langle \left\langle [S_{i\alpha}^z, \mathcal{H}_{df}]_- c_{k\gamma m''\sigma}; c_{j\beta m'\sigma}^+ \right\rangle \right\rangle_E \xrightarrow{n \rightarrow 0} 0, \\ & \left\langle \left\langle [S_{i\alpha}^{-\sigma}, \mathcal{H}_{df}]_- c_{k\gamma m''-\sigma}; c_{j\beta m'\sigma}^+ \right\rangle \right\rangle_E \xrightarrow{n \rightarrow 0} 0. \end{aligned}$$

Hence, for the equations of motion of the Ising and the Spin-flip function we get

$$\begin{aligned} & \sum_{l\delta m'''} \left(E \delta_{kl} \delta_{\gamma\delta} \delta_{m''m'''} - T_{kl\gamma\delta}^{m''m'''} \right) \Gamma_{ilj\alpha\delta\beta\sigma}^{m''m'}(E) \\ & = \hbar \langle S_{i\alpha}^z \rangle \delta_{kj} \delta_{\gamma\beta} \delta_{m''m'} + \\ & + \left\langle \left\langle S_{i\alpha}^z [c_{k\gamma m''\sigma}, \mathcal{H}_{df}]_- ; c_{j\beta m'\sigma}^+ \right\rangle \right\rangle_E \end{aligned} \quad (36)$$

$$\begin{aligned} & \sum_{l\delta m'''} \left(E \delta_{kl} \delta_{\gamma\delta} \delta_{m''m'''} - T_{kl\gamma\delta}^{m''m'''} \right) F_{ilj\alpha\delta\beta\sigma}^{m''m'}(E) \\ & = \left\langle \left\langle S_{i\alpha}^{-\sigma} [c_{k\gamma m''-\sigma}, \mathcal{H}_{df}]_- ; c_{j\beta m'\sigma}^+ \right\rangle \right\rangle_E. \end{aligned} \quad (37)$$

On the right-hand side of these equations appear further higher Green functions which prevent a direct solution and require an approximative treatment. The treatment is different for the

non-diagonal terms, $(i, \alpha, m) \neq (k, \gamma, m'')$ and for the diagonal terms, $(i, \alpha, m) = (k, \gamma, m'')$. In the first case we use a self-consistent so-called *self-energy approach* which results in a decoupling of the equations of motion. For the diagonal terms, $(i, \alpha) = (k, \gamma)$, this approach is replaced by a moment technique which takes the local correlations better into account.

The details of the approach have already been published in our previous paper⁷. By introducing the multi-indices A, B, \dots , defined by $(\alpha, m) \rightarrow A$, $(\beta, m') \rightarrow B, \dots$, the approximative solution for the electronic subsystem of the single-band KLM presented in⁷ can be transferred to the case of the multi-band KLM, with the correspondence $\alpha \cong A$, $\beta \cong B, \dots$

The reason for this straightforward transference is that the commutator relations which govern the solution in⁷ are invariant under the index transition, e.g.

$$\begin{aligned} [c_{i\alpha\sigma}, H_{sf}^{sb}]_- &= -\frac{J}{2} (z_\sigma \mathbf{S}_{i\alpha}^z c_{i\alpha\sigma} + \mathbf{S}_{i\alpha}^{-\sigma} c_{i\alpha-\sigma}) \\ [c_{iA\sigma}, H_{df}^{mb}]_- &= -\frac{J}{2} (z_\sigma \mathbf{S}_{i\alpha}^z c_{i\alpha m\sigma} + \mathbf{S}_{i\alpha}^{-\sigma} c_{i\alpha m-\sigma}) \\ &= -\frac{J}{2} (z_\sigma \mathbf{S}_{iA}^z c_{iA\sigma} + \mathbf{S}_{iA}^{-\sigma} c_{iA-\sigma}) \end{aligned} \quad (38)$$

Thus there is no need to repeat the procedure once more. For details the reader is referred to⁷

IV. RESULTS FOR EUO-FILMS

EuO crystallizes in the NaCl structure. Hence, the Eu^{2+} ions are arranged on an fcc lattice. For all the following film calculations, we assume the surface to be parallel to the fcc(100) crystal plane.

A. Magnetic properties

The calculation of the magnetic properties of the EuO films has been done with the theory of Sect.III.A. We take the Heisenberg-exchange integrals from the experiment. Low temperature neutron scattering measuring the spin-wave dispersion³⁸ and being compared to the renormalized spin wave theory³⁹ have revealed that nearest (J_1) and next-nearest neighbor (J_2) exchange integrals have to be taken into account:

$$\begin{aligned} \frac{J_1}{k_B} &= 0.625 K \\ \frac{J_2}{k_B} &= 0.125 K \end{aligned} \quad (39)$$

For an fcc (100) film, we have therefore for the case of uniform J_1 and J_2 within the film:

$$\begin{aligned} J_{ij}^{\alpha\beta} &= J_1 (\delta_{i,j+\Delta_{1\parallel}}^{\alpha\beta} + \delta_{i,j+\Delta_{1\perp}}^{\alpha\beta\pm 1}) \\ &+ J_2 (\delta_{i,j+\Delta_{2\parallel}}^{\alpha\beta} + \delta_{i,j}^{\alpha\beta\pm 2}) \end{aligned} \quad (40)$$

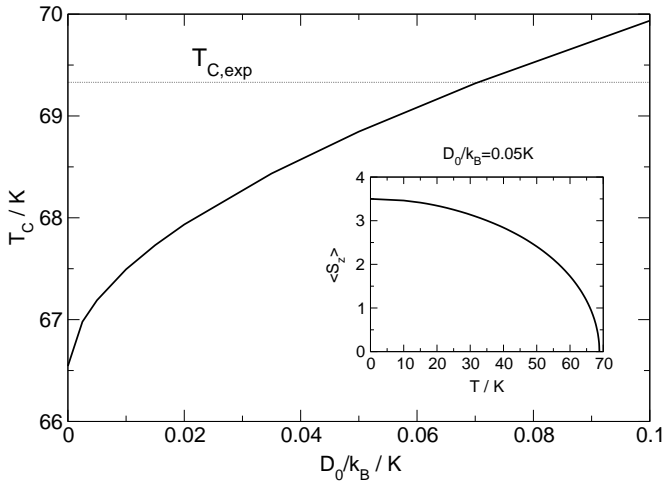


FIG. 5: Dependence of the Curie temperature T_C on the single-ion anisotropy constant D_0 , calculated for bulk EuO. Dotted line represents the experimental value, $T_C = 69,33\text{K}$. Inset: Magnetization of bulk EuO as function of temperature, calculated for $D_0 = 0.005k_B$

Here, $\Delta_{1\parallel}$, $\Delta_{1\perp}$ and $\Delta_{2\parallel}$ denote, respectively, the positions of nearest neighbors within the same layer, within the adjacent layers and of next-nearest neighbors within the same layer one finds,

$$\begin{aligned} 2\Delta_{1\parallel} &= (1, 1), (1, -1), (-1, 1), (-1, -1) \\ 2\Delta_{1\perp} &= (0, 1), (0, -1), (1, 0), (-1, 0) \\ \Delta_{2\parallel} &= (0, 1), (0, -1), (1, 0), (-1, 0) \\ \Delta_{2\perp} &= (0, 0) \end{aligned} \quad (41)$$

It remains to fix in a reasonable manner the single-ion anisotropy constant D_0 . For this purpose we have calculated the Curie temperature of bulk (!) EuO with J_1, J_2 from (41) and variable D_0 . The result is shown in Fig. 5. When $\frac{D_0}{k_B}$ increases from 0 to 0.1K T_C rises from about 66.5K to 70K. Regarding that J_1, J_2 stem from a low-temperature fit, the agreement between the calculated T_C 's and the experimental value of 69.33K³ is remarkably good and that for all D_0 -values in the investigated region. We have chosen $\frac{D_0}{k_B} = 0.05\text{K}$ for our calculations of film geometries. This is in reasonable agreement with the rather sparse experimental values. According to (20) and (21) the model anisotropy energy is $E_a = -D_0 \Phi_\alpha$ with the temperature-dependent anisotropy coefficient Φ_α from Eq. (22). It can be seen that E_a monotonically decreases as function of $\langle S_\alpha^z \rangle$ to $E_a = -6D_0$ at $\langle S_\alpha^z \rangle = S$. That means at $T = 0$ we have $\frac{E_a}{k_B} \approx -0.3$ which is the same order of magnitude as the experimental value in ref.⁴⁰.

Fig. 6 shows the temperature and layer-dependent magnetizations of EuO(100) films for thicknesses from $n = 1$ to $n = 20$. For all temperatures and for all film thicknesses the $\langle S_\alpha^z \rangle$ increase from the lowest magnetization of the surfaces monotonously towards the highest magnetizations in the film centers. That can qualitatively be explained by the lower coordination number of the surface atoms, $Z_{S,fcc(100)} = 4$, com-

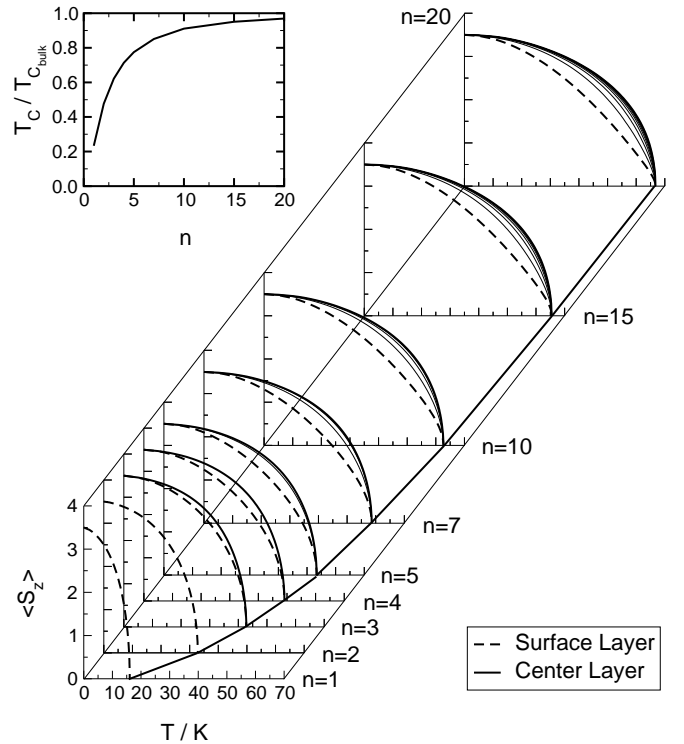


FIG. 6: Layer-dependent magnetizations, $\langle S_\alpha^z \rangle$, of EuO(100) films as functions of temperature for various thicknesses n . $\langle S_\alpha^z \rangle$ always increases monotonously from the surface layer towards the film center. Inset: Curie temperature as a function of film thickness.

pared to the bulk coordination number, $Z_{b,fcc} = 12$. The inset of Fig. 6 shows the dependence of the Curie temperature on the film thickness n compared to the bulk- T_C calculated with the same parameters J_1, J_2 , and D_0 (see inset of Fig. 5). Starting from a rather low value for the monolayer T_C steadily increases with n reaching the bulk-value for $n \geq 20$. The curve strongly resembles that of Gd films⁴¹. Corresponding measurements for EuO are unknown to us.

All the higher spin correlation functions $\langle S_\alpha^\pm S_\alpha^\mp \rangle$, $\langle (S_\alpha^z)^2 \rangle$, $\langle (S_\alpha^z)^3 \rangle$, ... follow from $\langle S_\alpha^z \rangle$ via (18), (23), (24). Examples are plotted in Fig. 2 of ref.⁷. Together with $\langle S_\alpha^z \rangle$ they provide the necessary temperature information needed to calculate the temperature-dependent electronic structures of EuO films, which are presented in the next Section.

B. Temperature-dependent electronic structure

In order to get the temperature-dependent band structures of the EuO(100) films we have to combine the LSDA calculations, described in Sect.II.B, with the many-body evaluation of the multiband-Kondo lattice model (Sect.III.B). It has been shown in previous works^{5,6,7} that the d-f exchange interaction of the KLM can be treated exactly for $T=0$ in the case of empty conduction bands. While the \downarrow -spectrum turns out to be rather complicated exhibiting interesting correlation effects, the \uparrow -spectrum is simple being only slightly shifted towards lower

energies by a constant energy amount of $\frac{1}{2}JS$. So we can directly use the TB-LMTO obtained \mathbf{k} -dependent hopping matrices for the \uparrow -electron as input for the single-particle Hamiltonian H_d (3). The problem of double-counting of relevant interactions, here the d-f-exchange interaction, which usually occurs when combining first-principles and model calculations, is then elegantly avoided. The temperature comes into play via the layer- and temperature-dependent f-spin correlation functions, discussed in the last section, which appear in the many-body evaluation of the KLM (Sect. III B). To avoid ambiguities, we use in the following as temperature-parameter the reduced magnetization $\frac{\langle S_z^z \rangle}{S}$ of the center layer of the respective EuO (100) film. The same temperature may produce in the other layers different magnetizations.

Table I gives some examples how the different values of the magnetization $\frac{\langle S_z^z \rangle}{S}$ are related to the respective temperatures for EuO (100) films. The only parameter of our theory, the exchange coupling J , is chosen from bulk-EuO calculations⁴² to yield the experimentally observed ‘red shift’ of the lower conduction band edge upon cooling down from $T = T_C$ to $T = 0$:

$$J = 0.25 \text{ eV} \quad (42)$$

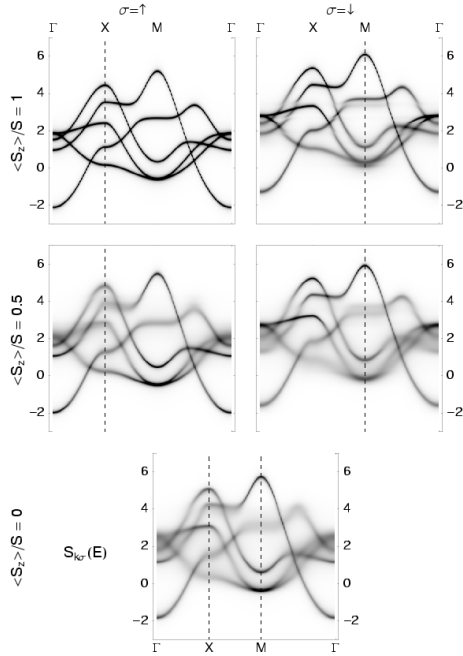


FIG. 7: Spin-dependent spectral densities of the Eu-5d bands of a EuO(100) monolayer for different magnetizations $\langle \frac{S_z^z}{S} \rangle$ (see Table I).

$\langle S_z^z \rangle/S$	bulk EuO	EuO(100) films (number of layers)				
		1	2	5	10	20
1	0	0	0	0	0	0
0.75	45.48	10.52	21.56	37.41	43.23	45.14
0.5	59.76	13.95	28.51	47.51	55.59	58.92
0.25	66.71	15.56	31.82	52.02	61.02	65.04
0 (T_C)	68.84	16.06	32.83	53.36	62.70	66.73

TABLE I: Temperatures at which the 4f magnetization of bulk EuO and of the center layers of EuO (100) films has assumed the values in the left column (see Figs. 5, 6)

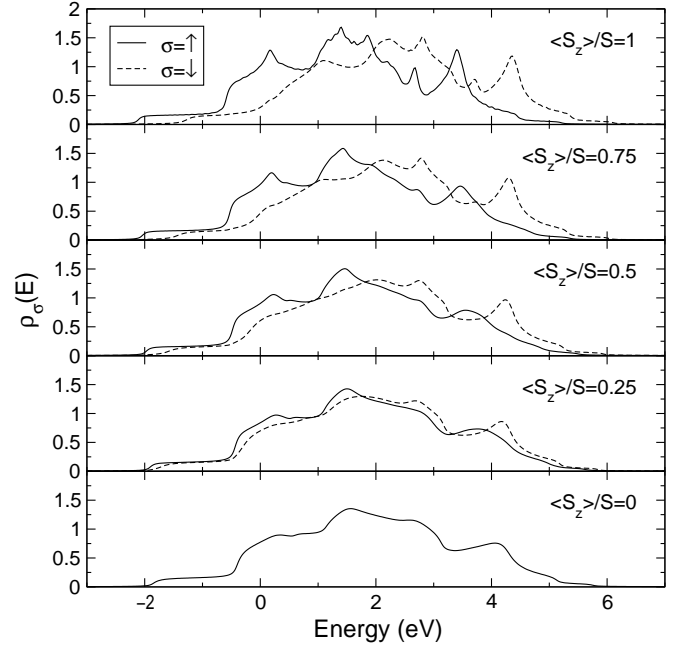


FIG. 8: Temperature-dependent densities of states of the Eu-5d bands of a EuO(100) monolayer for different values of the 4f magnetization $\langle \frac{S_z^z}{S} \rangle$ (see Table I).

Let us start the discussion with the spectral densities and the quasiparticle densities of states (Q-DOS) of the Eu-5d bands for a EuO(100) monolayer ($n=1$) at varying magnetizations $\frac{\langle S_z^z \rangle}{S}$ of the 4f moment system. Fig. 7 shows the quasiparticle band structure as a density plot. The degree of blackening is a measure of the peak-height of the respective spectral density. Broad, washed out lines mean quasiparticles with relatively low life-times. In ferromagnetic saturation ($\frac{\langle S_z^z \rangle}{S} = 1$) the \uparrow -spectrum consists of stable quasiparticles. As explained above this is the exactly solvable limiting case. The spectrum is identical to the LSDA input only slightly shifted by $-\frac{1}{2}JS$. The \downarrow -spectrum is also exactly solvable exhibiting, however, clear correlation effects as, e.g., a splitting of the dispersion around 4eV near the M-points. As discussed in detail for a model system in ref.^{5,7} the two excitations belong to two different microscopic interaction processes. The high-energy part is due to the formation of a magnetic polaron (propagating electron ‘dressed’ by a virtual cloud of magnons), the low-energy branch is due to scattering processes (magnon-emission by the

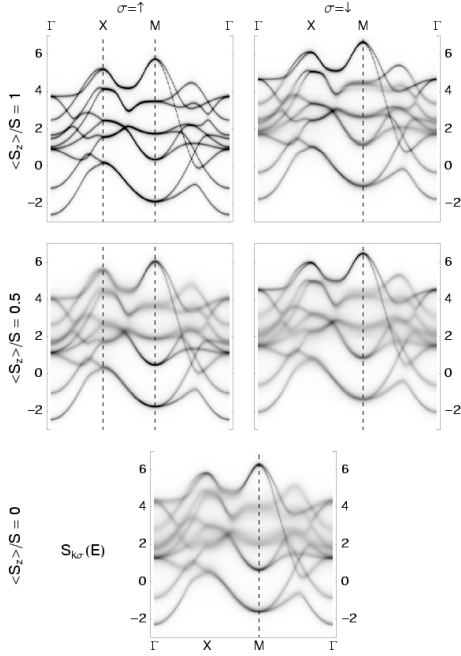


FIG. 9: Spin-dependent spectral densities of the Eu-5d bands of an EuO(100) double layer ($n=0$) for different values of the 4f magnetization $\langle \frac{S_z}{S} \rangle$ (see Table I).

\downarrow -electron). The magnetic polaron can be considered as due to a polarization of the neighboring 4f spins by the conduction electron via d-f exchange. Under certain parameter constellations this may even lead to a bound state, e.g. to a quasiparticle with infinite lifetime^{5,7}. This exchange-induced splitting, which can also be observed in other parts of the $T=0$ - \downarrow -band structure, is a typical correlation effect, which by no means can be accounted for in an LSDA calculation.

An exchange splitting of the full \uparrow - and \downarrow spectra against one another is clearly visible. Note that these effects appear although the bands are empty, more strictly there is one electron ('test electron') in the otherwise empty 5d-bands. They are therefore certainly induced by the 4f system and mediated by the d-f exchange interaction.

For finite temperature, intermediate magnetizations, $\frac{\langle S_z \rangle}{S} = 0.5$, the \uparrow -dispersion, too, starts to wash out indicating spin-flip processes. Magnon emission by a \downarrow -electron is completely equivalent to magnon absorption by a \uparrow -electron, with one exception: magnon absorption is possible only if there are any in the spin system. This is not the case in ferromagnetic saturation ($\langle S_z \rangle = S$). That is the reason why at $T=0$ K the \uparrow -spectrum appears so much simpler than the \downarrow -spectrum. For

finite temperatures (demagnetizations) magnons are available, absorption processes lead to damping of the quasiparticle dispersion in the \uparrow -spectrum, too. The overall exchange splitting reduces with increasing temperatures and the two spin spectra are becoming more and more similar. Finally, in the limit of $\langle S_z \rangle \rightarrow 0$, $T \rightarrow T_C$ the lack of any 4f-magnetization removes the induced spin-asymmetry in the 5d bands (Fig. 7).

The temperature-dependent Q-DOS of the EuO-5d bands in a monolayer exhibits a strong induced exchange splitting at $T=0$ (Fig. 8), where the increase of temperature from $T=0$ to $T = T_C$ leads to a convergence of the two spin parts. It can clearly be seen that the temperature dependence of the exchange-split spectra goes beyond the Stoner picture, where the bands move rigidly towards each other when the temperature is increased. The reason lies predominantly in the spin-flip processes between 5d- and 4f- system. Such correlation effects take care for the non-rigid shift. By comparison with the \uparrow -Q-DOS for ferromagnetic saturation ($\langle S_z \rangle = S$), the shape of which is identical to the LDA-renormalized single-particle input, one recognizes that in the paramagnetic phase, too, correlation effects remarkably alter the spectrum.

Fig. 9 displays the spectral density of a EuO double layer for three different magnetizations of the 4f-moment system. The same which has been said above about the temperature-dependent tendencies of the monolayer EuO(100) spectra applies to the spectra of the double-layer in Fig. 9. However, due to the higher number of bands which originates from the hybridization of the two EuO(100) layers the temperature-dependent evolution of the bands becomes less clear for the

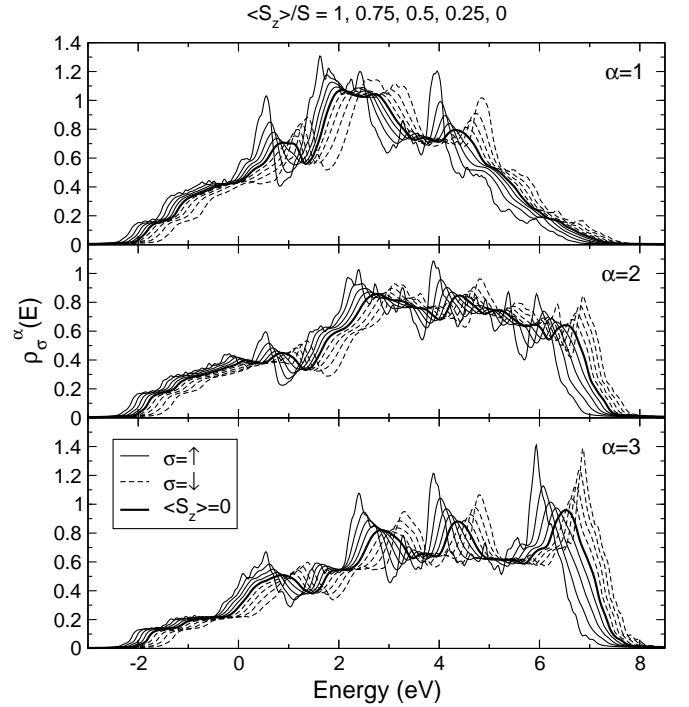


FIG. 10: Local densities of states of the Eu-5d bands of the first, second and center layer of a 5-layer EuO(100) film for different values of the center layer 4f magnetization $\langle \frac{S_z}{S} \rangle$ (see Table I).

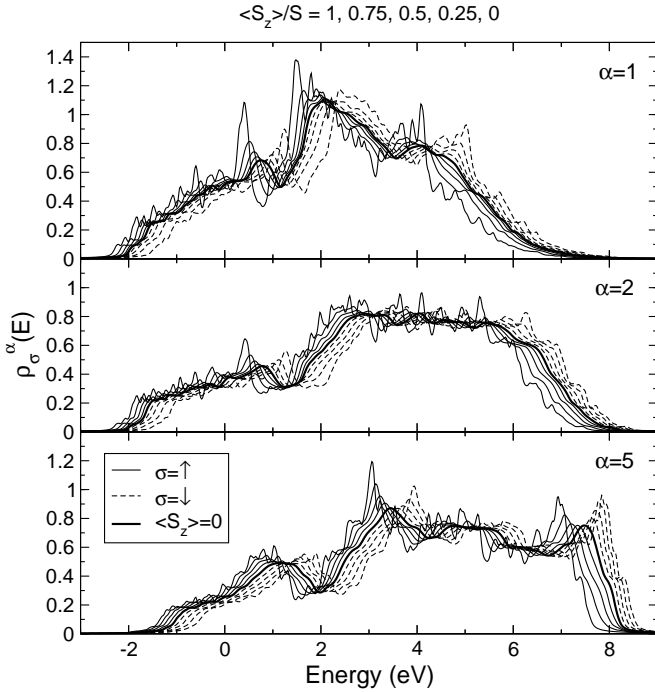


FIG. 11: The same as in Fig. 10 but for a 10-layer film

EuO(100) double layer.

Figs. 10 and 11 show the temperature-dependent Q-DOS of, respectively, a 5-layer and a 10-layer EuO(100) film. Different from the case of the monolayer and the double layer, for these films the densities of states depend on the layer index α . Furthermore, the magnetization of the 4f-moment system is a layer-dependent entity (see Fig. 6). Here, the temperature parameter $\frac{\langle S_z \rangle}{S}$ refers to the magnetization of the center layer of the film. The respective temperatures are given in Table I.

With increasing film thickness, the Q-DOS of the center layer becomes more and more similar to the Q-DOS of bulk EuO. As a result, the centers of gravity of the surface layer bands, on the one hand, and of the center layers, on the other hand, move away from each other, with the latter positioning at higher energies. This tendency leads to the existence of EuO(100) surface states, which are discussed in detail in an additional paper³⁴.

There it is shown that for $T = T_C$ the surface at the Γ -point lies some 0.8 eV below the bulk conduction band edge. This distance does not change with temperature, t.e. the \uparrow part of the surface state exhibits the same red shift of about 0.3 eV as the 5d conduction band edge when cooling down to $T_C = 0$ K. Since the paramagnetic 4f–5d gap amounts to 1.12 eV³ it can be speculated³⁴ that the \uparrow -surface state closes the gap at very low temperatures. Giving rise to a temperature-induced surface insulator–halfmetal transition. The Eu-ion then remains in an intermediate valence fluctuating between the magnetic 4f⁷-state ($J = S = \frac{7}{2}$) and the non-magnetic 4f⁶-state ($J = 0$). Interesting dynamic effects are to be expected since the non-magnetic 4f⁶-state automatically cancels the red shift pushing the \uparrow -surface states by 0.3 eV to higher

energies. Electrons which will reenter the 4f level creating again the magnetic 4f⁷ configuration, and so on.

V. CONCLUSIONS

By combination of a ‘first-principles’ band structure calculation within the frame of density functional theory with a many-body evaluation of a proper theoretical model we have derived the temperature-dependent electronic structure and the magnetic properties of a real 4f system (EuO) with film geometry. The theory provides the properties of films of varying thicknesses. The film geometry provokes a superposition of electron correlation effects with the sheer geometrical dependence of the spectra on film thickness and layer index.

‘Local-moment’ systems like EuO get their striking temperature dependencies and correlation effects by an exchange interaction between localized magnetic moments, due to 4f electrons of the Rare Earth ion, and quasi-free (5d,6s) conduction electrons. The situation is rather convincingly modeled by the Kondo-lattice (s-f, s-d) model (KLM). We proposed a way how to generalize the original single-band KLM to a realistic multi-band model. The respective many-body problem is approximately solved for the electronic subsystem making use of a moment-conserving decoupling approximation (MCDA) for suitably defined Green functions. The method gains substance by the fact that the finite-temperature theory evolves continuously from the exactly solvable and nontrivial $T=0$ case of ferromagnetic saturation.

The mentioned $T=0$ -limiting case is also used to connect the multiband-model treatment with a TB-LMTO-ASA band structure calculation for thin EuO(100) films. Circumventing the much discussed double-counting problem the spin-up Eu-5d bands have been taken as input for the hopping matrix of the multi-band-KLM Hamiltonian. The reason is that the exact $T=0$ -KLM solution shows for ferromagnetic saturation that the \uparrow -quasiparticle spectrum is only rigidly shifted compared to the ‘free’ dispersions. A double counting of the d-f exchange interaction is therefore excluded.

The film geometries are accounted for by a supercell construction, where consecutive EuO(100) films are isolated from each other by a stack of spacer layers. The connection to the model calculation employs a decomposition into subbands, that respects the symmetry of the Eu-5d orbitals.

Already for the case of ferromagnetic saturation of the 4f-moment system, the spin-down spectra of the EuO films exhibit strong deviations from the single-electron LSDA results demonstrating strong correlation effects. These correlation effects in the \downarrow -spectra provoke a strong temperature-dependence. The \uparrow -spectra, which at $T=0$ correspond to the \uparrow -LSDA band structure results, develop similar correlation effects for finite temperatures. The loss of 4f magnetization for $T \rightarrow T_C$ leads to a convergence of the spectra for both spin directions.

The semiconductor EuO fits the physics of the KLM for the special case of an empty conduction band. The extension to non-zero band occupation allows to study the prototypical ‘local moment’ metal Gd. Concerning the aspect of re-

duced dimensionality, the dependence of magnetic and electronic properties of Gd films are of high experimental and theoretical interest. Respective forthcoming investigations will shed light on some extraordinary physical properties of the lanthanides, in particular the enhanced Curie temperature of the Gd(0001) surface and its relation to the temperature behavior of the Gd(0001) surface state.

Acknowledgment

Financial support by the ‘Sonderforschungsbereich 290’ and by the German Merit Foundation is gratefully acknowledged.

-
- * Email: Wolf.Mueller@physik.hu-berlin.de; URL: <http://tfk.physik.hu-berlin.de>
- ¹ A. P. Ramirez, *J. Phys. C* **9**, 8171 (1997).
 - ² S. Legfold, ‘Ferromagnetic Materials’ vol. **1** chapter 3, (E. P. Wohlfarth Amsterdam, North Holland 1980).
 - ³ P. Wachter, ‘Handbook of Physics and Chemistry of Rare Earths’, vol. **1** chapter 19, (K. A. Gschneidner and L. Eysing Amsterdam, North Holland 1979).
 - ⁴ T. Penney, M.W. Schafer, J.B. Torrance, *Phys. Rev. B* **5**, 3669 (1972).
 - ⁵ W. Nolting, S. Rex and S. Mathi Jaya, *Phys. Rev. B* **54**, 14455 (1996).
 - ⁶ W. Nolting, S. Mathi Jaya and S. Rex, *J. Phys. B* **9**, 1301 (1997).
 - ⁷ R. Schiller and W. Nolting, *Phys. Rev. B* **60**, 462 (1999).
 - ⁸ J. Schoenes and P. Wachter, *Phys. Rev. B* **9**, 3097 (1974)
 - ⁹ C. Godart et al., *J. Physique* **41**, C5-263 (1980).
 - ¹⁰ C. Zener, *Phys. Rev.* **81**, 440 (1951).
 - ¹¹ W. Nolting, *phys. stat. sol. (b)* **96**, 11 (1979).
 - ¹² N. Furukawa, *J. Phys. Soc. Japan* **63**, 3214 (1994).
 - ¹³ N. Furukawa, *cond-mat* 9812066 (1998).
 - ¹⁴ E. Dagotto, S. Yunoki, A. L. Malvezzi, A. Moreo, J. Hu, S. Capponi, D. Poilblanc and N. Furukawa, *Phys. Rev. B* **58**, 6414 (1998).
 - ¹⁵ N. Grewe and F. Steglich, ‘Handbook of Physics and Chemistry of Rare Earths’, vol. **14**, (K. A. Gschneidner and L. Eysing Amsterdam, Elsevier 1991).
 - ¹⁶ D. Weller, S. F. Alvarado, W. Gudat, K. Schröder and M. Campagna, *Phys. Rev. Lett.* **54**, 1555 (1985).
 - ¹⁷ C. Rau and S. Eichner, *Phys. Rev. B* **34**, 6347 (1986).
 - ¹⁸ H. Tang, D. Weller, T. G. Walker, J. C. Scott, C. Chappert, H. Hopster, A. W. Pang, D. S. Dessau and D. P. Pappas, *Phys. Rev. Lett.* **71**, 444 (1993).
 - ¹⁹ M. Donath, B. Gubanka, F. Passek, *Phys. Rev. Lett.* **77**, 5138 (1996)
 - ²⁰ C.S. Arnold, D.P. Pappas, *Phys. Rev. Lett.* **85**, 5202 (2000)
 - ²¹ R. Wu and A. J. Freeman, *J. Magn. Mater.* **99**, 81 (1991).
 - ²² D. Li, C. W. Hutchings, P. A. Dowben, C. H. Wang, R. - T. Wu, M. Onellion, A. B. Andrews and J. L. Erskine, *J. Magn. Mater.* **99**, 85 (1991).
 - ²³ A. V. Fedorov, K. Starke and G. Kaindl, *Phys. Rev. B* **50**, 2739 (1994).
 - ²⁴ E. Weschke, C. Schüssler-Langheine, R. Meier, A. V. Fedorov, K. Starke, F. Hübinger and G. Kaindl, *Phys. Rev. Lett.* **77**, 3415 (1996).
 - ²⁵ M. Donath, P. A. Dowben and W. Nolting, editors, ‘Magnetism and Electronic Correlations in Local-Moment Systems: Rare Earth Elements and Compounds’, (World Scientific, Singapore 1998).
 - ²⁶ N. M. Mermin and H. Wagner, *Phys. Rev. Lett.* **17**, 1133 (1966).
 - ²⁷ A. Gelfert and W. Nolting, *phys. stat. sol. (b)* **217**, 805 (2000).
 - ²⁸ K. Held and D. Vollhardt, *Phys. Rev. Lett.* **84**, 5168 (2000).
 - ²⁹ O. K. Andersen, *Phys. Rev. B* **12**, 3060 (1975).
 - ³⁰ O. K. Andersen and O. Jepsen, *Phys. Rev. Lett.* **53**, 2571 (1984).
 - ³¹ O. Eriksson, R. Ahuya, A. Ormeci, J. Trygg, O. Hjortstam, P. Söderlind, B. Johansson and J. M. Wills, *Phys. Rev. B* **52**, 4420 (1995).
 - ³² V. I. Anisimov, J. Zaanen and O. K. Andersen, *Phys. Rev. B* **44**, 943 (1991).
 - ³³ V. I. Anisimov, F. Aryasetiawan and A. I. Lichtenstein, *J. Phys. : Condens. Matter* **9**, 767 (1997).
 - ³⁴ R. Schiller and W. Nolting, *Phys. Rev. Lett.*, **86**, 3847 (2001)
 - ³⁵ M. E. Lines, *Phys. Rev.* **156**, 534 (1967).
 - ³⁶ R. Schiller and W. Nolting, *Solid State Commun.* **110**, 121 (1999).
 - ³⁷ H. B. Callen, *Phys. Rev.* **130**, 890 (1963).
 - ³⁸ H. C. Bohn, W. Zinn, B. Dorner and A. Kollmar, *Phys. Rev. B* **22**, 5447 (1980).
 - ³⁹ W. Nolting, ‘Quantentheorie des Magnetismus’ Teil 2: Modelle, (Teubner, Stuttgart 1986).
 - ⁴⁰ N. Miyata and B. E. Argyb, *Phys. Rev.* **157**, 448 (1967).
 - ⁴¹ M. Farle, K. Baberschke, U. Stetter, A. Aspelmeier and F. Gerhardter, *Phys. Rev. Lett.* **47**, 11571 (1993).
 - ⁴² R. Schiller and W. Nolting, *Solid State Commun.* **118**, 173 (2001)